Life Sciences 122 (2015) 15–25

Contents lists available at ScienceDirect

Life Sciences

journal homepage: www.elsevier.com/locate/lifescie

# Luteolin inhibits ROS-activated MAPK pathway in myocardial ischemia/reperfusion injury

Dongsheng Yu [a], Mengwen Li [a], Youqing Tian [b], Jun Liu [a], Jing Shang [a,c,*]

[a] Center for Drug Screening & State Key Laboratory of Natural Medicines, China Pharmaceutical University, 24 Tong Jia Xiang, Nanjing 210009, PR China
[b] Lianyungang TCM Branch, Jiangsu Union Technical Institute, Lianyungang 222007, PR China
[c] Qinghai Key Laboratory of Tibetan Medicine Pharmacology and Safety Evaluation, Northwest Institute of Plateau Biology, Chinese Academy of Sciences, Xining 810008, PR China

ARTICLE INFO

*Article history:*
Received 9 May 2014
Accepted 8 November 2014
Available online 2 December 2014

*Keywords:*
Luteolin
Myocardial ischemia/reperfusion injury
Reactive oxygen species
MAPK
Mitochondrial
Apoptosis

ABSTRACT

*Aims:* Luteolin is a falconoid compound that has an antioxidant effect, but its contribution to ROS-activated MAPK pathways in ischemia/reperfusion injury is seldom reported. Here, we have confirmed that it exhibits an antioxidant effect in myocardial ischemia/reperfusion injury (MIRI) by inhibiting ROS-activated MAPK pathways.
*Main methods:* We exposed rat hearts into the left anterior descending coronary artery (LAD) ligation for 30 min followed by 1 h of reperfusion. Observations were carried out using electrocardiography; detection of hemodynamic parameters; and testing levels of lactate dehydrogenase (LDH), creatine kinase (CK), total superoxide dismutase (T-SOD), and malondialdehyde (MDA). Mitogen-activated protein kinase (MAPK) pathway was measured by western blot and transmission electron microscopy was applied to observe the myocardial ultrastructure. Rat H9c2 cell in 95% $N_2$ and 5% $CO_2$ stimulated the MIRI. Oxidation system mRNA levels were measured by real-time PCR; mitochondrial membrane potential and apoptosis were measured by confocal microscopy and flow cytometry; western blot analysis was used to assay caspase-3, -8, and -9 and MAPK pathway protein expression; the MAPK pathway was inhibited using SB203580 (p38 MAPK inhibitor) and SP600125 (c-Jun $NH_2$-terminal kinase inhibitor) before H9c2 cells were exposed to hypoxia/reoxygenation injury to show the modulation of the changes in ROS generation, cell viability and apoptosis.
*Key findings:* In vivo, luteolin can ameliorate the impaired mitochondrial morphology, regulating the MAPK pathway to protect MIRI. In vitro, luteolin can affect the oxidation system, mitochondrial membrane potential and MAPK pathway to anti-apoptosis.
*Significance:* These results reveal a ROS–MAPK mediated mechanism and mitochondrial pathway through which luteolin can protect myocardial ischemia/reperfusion injury.



## Introduction

Ischemic heart disease (IHD) is the leading cause of death of cardiovascular disease (CVD), and IHD associated with mortality accounted for 42% of CVD [1]. Prevention and management of myocardial ischemia/reperfusion injury (MIRI) is a key step in coronary heart disease surgery [2] and is becoming a major clinical problem of IHD treatment [3]. The mechanism of MIRI is very complex, the currently accepted theories include energy metabolism, free radicals, calcium overload, neutrophil infiltration, and vascular endothelial dysfunction [4], eventually resulting in apoptosis or necrosis.

Ischemia-mediated damage to the mitochondrial electron transport chain persists during reperfusion [5], while mitochondria is an important subcellular organelle for the cellular oxidative process and also the main source of reactive oxygen species in the cell [6], the mitochondrial dysfunction decreases energy production [7], increases the generation of reactive oxygen species (ROS) [8,9], and favors executioner caspase cleavage pathway activation to trigger myocardial cell death during reperfusion [10].

ROS can activate the mitogen-activated protein kinase (MAPK) pathway [11], which has a pivotal role in cardiovascular disease and MIRI process of signal transduction has a pivotal role [12]. ERK1/2 activation is involved in cell-survival and the recovery of damaged myocardium ischemia while JNK and p38 participate in myocardial apoptosis [13]. MAPK kinases can promote the release of cytochrome *c* and eventually result in apoptosis [14].

Luteolin, 3′,4′,5,7-tetrahydroxyflavone, is a falconoid compound that can be found in many traditional Chinese medicines, with anti-inflammatory [15], anti-oxidant [16], and anti-tumor [17] effects. In recent years, it has been applied in pharmacological and clinical practice for the prevention of IHD and MIRI [18], but its molecular target for prevention and treatment of MIRI requires further research. Luteolin acts by correcting oxidant/antioxidant imbalance, significantly attenuating

* Corresponding author at: Center for Drug Screening & State Key Laboratory of Natural Medicines, China Pharmaceutical University, 24 Tong Jia Xiang, Nanjing 210009, PR China. Tel.: +86 25 83271057; fax: +86 25 83271142.
*E-mail address:* shangjing21cn@163.com (J. Shang).

http://dx.doi.org/10.1016/j.lfs.2014.11.014
0024-3205/

increases in ROS production and preventing decreases in mitochondrial activities on neurons, and inhibiting HGF-induced HepG2 cell invasion involving the MAPK/ERK pathway. While the ROS significantly mediates the MAPK pathway effect lots in MIRI [19–21], it ultimately induces mitochondria damage.

Our supposition was that luteolin can have a myocardial protection effect on MIRI by ROS–MAPK pathway and mitigate mitochondrial dysfunction. With the classic left anterior descending coronary artery ligation model and H9c2 cell nitrogen-induced hypoxia/reoxygenation model, we studied the protective effect of luteolin on myocardial ischemia/reperfusion injury in vivo and in vitro, respectively. The purpose of this study is to investigate whether pretreatment with luteolin can reduce myocardial damage in MIRI.

## Materials and methods

### *Materials*

Luteolin compounds were supplied by Shanxi Huike Botanical Development Company, China, its purity (>98%) was determined by HPLC, slightly soluble in water and have the molecular formula of $C_{15}H_{10}O_6$ with a molecular weight of 286.23. DMSO, 2,3,5-triphenyltetrazolium chloride (TTC), phenylmethylsulphonyl fluoride (PMSF) were obtained from Sigma-Aldrich (St. Louis, Missouri, USA). Prestained molecular mass markers were from Thermo Fisher Scientific (Waltham, MA, USA). Mitochondrial membrane potential assay kit with JC-1 was obtained from Invitrogen Life Technologies; annexin-V/PI apoptosis detection kit was from KeyGEN Biotech (Nanjing, China). Primers for the detection of Mn-SOD, HO-1, HSP27 and GAPDH were synthesized by Genscript Life Technology (Nanjing, China). Antibodies against p-p38 MAPK, p38, p-ERK1/2, ERK1/2, p-JNK (Thr183/Tyr185), JNK, caspase-3, cleaved caspase-3 (Asp175), caspase-8, cleaved caspase-8 (Asp387), caspase-9, and cleaved caspase-9 (Asp330) were from Cell Signaling Technology (MA, USA); p47-phox was from Santa Cruz (Texas, USA); β-actin antibody, and horseradish peroxidase-conjugated secondary antibodies were purchased from Sigma-Aldrich (MO, USA). Enhanced BCA protein assay kit and cell lysis buffer were from Beyotime Institute of Biotechnology (Haimen, Jiangsu, China). SP600125 and SB203580 were purchased from Sigma-Aldrich (St. Louis, Missouri, USA). Other reagents were of the highest quality obtainable.

### *Animals*

The experiments were performed in adherence with the National Institutes of Health Guidelines on the Use of Laboratory Animals and were approved by the Ethic Committee on Animal Care of China Pharmaceutical University (Approval ID: SCXK-(Su) 2011-0003) and performed in strict accordance with the guidelines of the "Principles of Laboratory Animal Care" (NIH Publication No. 80-23, revised in 1996). Adult male Sprague-Dawley (SD) rats (6–8 weeks old, weighting 250–300 g) were purchased from the Liaoning Changsheng Biotechnology Company (Liaoning, Certificate No. SCXK 2010-0001). All animals were acclimated for one week under the following conditions: the room temperature was 23 ± 1 °C. Humidity was 50 ± 5% with a 12-hour light/dark cycle (lights on at 6:00 a.m. and off at 6:00 p.m.). During this period, food and water were provided ad libitum.

### *Construction of I/R injury animal model and drug administration*

I/R injury animal model was constructed by LAD ligation for 30 min followed by 1 h reperfusion [22]. In brief, rats were anesthetized with 1 g/kg urethane (Qingxi, Shanghai, China), ventilated with a positive pressure respirator (TKR-200C, Jiangxi, China) at a stroke volume of 12 ml/kg and a rate of 60 strokes per minute with 95% $O_2$ and 5% $CO_2$. The chest was opened through a left thoracic incision between the second and fourth ribs. A 6–0 silk suture slipknot was placed at the distal 1/3 of the left anterior descending artery. A small glass tube was placed between the ligature and myocardial tissues. For the ischemia injury, the coronary artery was occluded by tightening the tension. After 30 min of ischemia, the slipknot was released, and the myocardium was reperfused for 1 h. Sham operated control rats underwent the same surgical procedures except that the suture placed under the left coronary artery was not tied. In the luteolin + I/R group, luteolin dissolved in 0.5% CMC-Na solution was given through intragastric for 5 days before operation, with the concentration of 10, 40, and 70 mg/kg respectively for the three luteolin pretreatment groups. 30 animals were included and randomly distributed into the sham, I/R, luteolin (10 mg/kg) + I/R, luteolin (40 mg/kg) + I/R, and luteolin (70 mg/kg) + I/R, with 6 animals in each group.

Cardiac function was continuously determined by electrocardiography (ECG) evaluation during the entire I/R period, and hemodynamic measurement was conducted immediately after electrocardiography as described previously [23], left ventricular systolic pressure (LVSP), left ventricular end-diastolic pressure (LVEDP), maximum rate of left ventricular pressure rise ($+dp/dt_{max}$) and maximum rate of left ventricular pressure decline ($-dp/dt_{min}$) were recorded and measured by a BL-420F polygraph system (Taimeng Technology Co., Ltd., Chengdu, China).

### *Tissue and serum preparation*

After reperfusion for 1 h, blood samples (500 μl) were collected from the eyeball of rat, and centrifuged at 1500 *g* for 10 min at 4 °C. Serum samples from the centrifuging process were transferred to Eppendorf tubes and stored at −80 °C until analyzed [24]. Part of heart specimens were harvested about 1 $mm^3$ fixed in 2.5% glutaraldehyde for ultrastructure detection; other specimens were partially fixed in 4% paraformaldehyde then embedded in paraffin-wax. The remaining heart specimens were wrapped in aluminum foil, deep frozen in liquid nitrogen.

### *Measurement of myocardial infarct size*

Myocardial infarct size was evaluated by TTC staining. After reperfusion, the hearts were immediately removed and sectioned into 5 mm thick short-axis slices from the apex towards the base of the heart. The slices were incubated in 1% TTC in PBS for 15–20 min at 37 °C and then photographed with a digital camera (Canon, Japan) [25]. Red parts in the heart, which were stained by TTC, represented for ischemic but viable tissue. White part areas indicated infarcted myocardium. Areas of infarct size were measured digitally using Image Pro Plus software.

### *Determination of serum lactate dehydrogenase (LDH), creatine kinase (CK), total superoxide dismutase (T-SOD), malondialdehyde (MDA)*

After reperfusion, orbital blood serum was collected by centrifugation at 1500 *g* for 10 min at 4 °C. The supernatant was used for assay of CK at 520 nm and leakage of myocardial lactate LDH at 450 nm was performed as described [26].

Detection of the T-SOD activity at 550 nm and MDA content was quantified by thiobarbituric acid assay with 1,1,3,3-tetramethoxypropane as an external standard at 532 nm according to the manufacturer's instructions [27]. Each measurement was performed in duplicate.

### *Myocardial ultrastructure*

Fresh myocardial tissues (1 $mm^3$) were excised from the surrounding infarction areas of the left ventricle after reperfusion. Tissues were fixed with 2.5% glutaric dialdehyde and post-fixed with 1% osmium tetroxide. The specimens were processed for ultrathin sections. The sections were stained with uranium acetate and lead citrate, and the

ultrastructural changes of myocardial tissue were then evaluated by a transmission electron microscope (H-7560, HITACHI, Japan) [28–30]. In each group, specimens were taken from six hearts and for each heart six tissue blocks were obtained.

*Cell culture and hypoxia/reoxygenation injury model [31]*

Rat H9c2 cardiomyocyte cell line was obtained from the American Type Culture Collection (ATCC, Manassas, VA, USA.). The H9c2 cells were maintained in high glucose DMEM supplemented with 10% (v/v) heat inactivated fetal bovine serum (FBS; Gibco/Invitrogen), 100 U/ml penicillin, 100 μg/ml streptomycin (Gibco/Invitrogen) at 37 °C in a humidified incubator with 5% $CO_2$.

When the H9c2 cells were cultured to 70–80% confluence, luteolin dissolved in DMSO into the medium with 5% FBS for the doses indicated for 24 h as luteolin treated group, control group and H/R group change medium with 5% FBS for 24 h. After that, all groups changed into Krebs-Ringer bicarbonate buffer (KRB; 115 mM NaCl, 4.7 mM KCl, 2.5 mM $CaCl_2$, 1.2 mM $KH_2PO_4$, 1.2 mM $MgSO_4$, 24 mM $NaHCO_3$, 10 mM HEPES; pH 7.4). Then the cells were cultured at 95% $N_2$ and 5% $CO_2$ anoxic environment for 6 h, changed into DMEM with 10% FBS and maintained at 5% $CO_2$, 95% air for 5 h as reoxygenation injury [32].

*Western blot evaluation*

After reperfusion, 100 mg myocardial tissue sample was taken from the infraction areas and preserved in liquid nitrogen before use. Cardiomyocytes were washed once in PBS and lysis buffer containing 20 mM Tris (pH 7.5), 150 mM NaCl, 1% Triton X-100, and 1 mM PMSF. Protein concentrations were determined by BCA protein assay kit. 50 μg proteins were resuspended in sample buffer containing 2% SDS, 2% β-mercaptoethanol, 50 mmol/l Tris–HCl (pH 6.8), 10% glycerol, and 0.05% bromophenol blue. Proteins were separated in a SDS-polyacrylamide gel and transferred to the PVDF membrane (Millipore Co., Bedford, USA). After blocking the membrane with Tris-buffered saline-Tween 20 (TBST, 0.1% Tween 20) containing 2.5% BSA for 1 h at room temperature, the membrane was washed twice with TBST and incubated with primary antibodies against p38 (CST9212, 1:1000 dilution), phospho-p38 (Thr180/Tyr182) (CST4631, 1:800 dilution), ERK1/2 (CST4695, 1:1000 dilution), phospho-ERK1/2 (Thr202/Tyr204) (CST4376, 1:800 dilution), JNK (CST9258, 1:1000 dilution), Phospho-JNK (Thr183/Tyr185) (CST9251, 1:800 dilution). The membranes were washed three times with TBST for 10 min and then incubated for 1 h at room temperature with 1:3000 dilution horseradish peroxidase (HRP)-conjugated secondary antibodies. After extensive washing, the bands were detected by enhanced chemiluminescence (ECL) reagent (Millipore Co., Bedford, USA). The band intensities were quantified using the ChemiDoc™ MP System (Bio-Rad, Hercules, USA).

H9c2 cell protein was extracted with RIPA buffer containing 1 mM PMSF; western blot protocol was the same with rat heart tissue samples. Rabbit anti-rat caspase-3 (CST9665, 1:1000 dilution), cleaved caspase-3 (Asp175) (CST9664, 1:1000 dilution), caspase-8 (CST4790, 1:1000 dilution), cleaved caspase-8 (Asp 387) (CST 8592, 1:1000 dilution), caspase-9 (CST9508, 1:1000 dilution), cleaved caspase-9 (Asp330) (CST7237, 1:1000 dilution), p47-phox (sc-7660, 1:1000 dilution) and MAPK pathway antibodies primary antibody were added to the membrane in TBST containing 2.5% BSA overnight at 4 °C. The secondary antibody, HRP-conjugated sheep anti-rabbit antibody, at a 1:3000 dilution in TBST containing 2.5% BSA, incubated at room temperature for 1 h. After extensive washing, the bands were detected by ECL reagent and quantified using the ChemiDoc™ MP System (Bio-Rad, Hercules, USA).

*Measurement of intracellular ROS accumulation*

2′,7′-dichlorodi-hydrofluorescein diacetate (DCFH-DA) was used to detect intracellular ROS level in H9c2 cells [33]. Briefly, H9c2 cells ($10^6$ cells/ml) were exposed to H/R injury in the presence and absence of luteolin, and rinsed once with PBS and then incubated with 25 μM DCFH-DA in DMEM without FBS at 37 °C for 30 min. After that, washed thrice with PBS, then the cells were collected and the 2′,7′-dichlorofluorescein (DCF) fluorescence was observed with Safire2 microplate reader (Tecan, Swiss) at an excitation wavelength of 488 nm and an emission wavelength of 525 nm.

*Real-time PCR*

Total RNA from H9c2 cells was extracted using TRIzol reagent (Invitrogen). RNA concentration was determined by a UV spectrophotometer. Real-time PCR amplifications were carried out using StepOnePlus™ Real-Time PCR System (Applied Biosystems, USA) and Thunderbird SYBR Master Mix (TOYOBO, Japan). Primer sequences were: Mn-SOD (forward: 5′-AAG GAG CAA GGT CGC TTA CAG A-3′, reverse: 5′-CAA ATG GCT TTC AGA TAG TCA GGT C-3′), HO-1 (forward: 5′-ATG AAC ACT CTG GAG ATG ACC CC-3′, reverse: 5′-GTC TGT GAG GGA CTC TGG TCT TTG-3′), HSP27 (forward: 5′-ACT GGC AAG CAC GAA GAA AGG-3′, reverse: 5′-AGG GGA CAG GGA AGA GGA CA-3′). Real-time PCR was performed with the following cycles: 95 °C for 10 min, followed by 95 °C for 15 s, 60 °C for 30 s, and 72 °C for 30 s for 40 cycles. GAPDH (forward: 5′-GAT CCC GCT AAC ATC AAA TG-3′, reverse: 5′-GAG GGA GTT GTC ATA TTT CTC-3′) expression was used as an internal control. $2^{-\Delta\Delta CT}$ was calculated for every sample, finally the mRNA expression levels were indicated with $2^{-\Delta\Delta CT}$ and normalized to GAPDH [34].

*Measurement of mitochondrial membrane potential (ΔΨm) levels*

Mitochondria of H9c2 cells were stained with JC-1 (5,5′,6,6′-tetrachloro-1,1′,3,3′-tetraethyl-benzimidazolylcarbocyanine iodide) [35]. Cells were incubated with JC-1 dissolved in DMEM without FBS at 37 °C for 30 min, then washed three times with PBS. The fluorescence of the cell was measured at an excitation wavelength of 507 nm and an emission wavelength of 529 nm by a confocal laser scanning microscope (Olympus FV 1000).

*H9c2 cell apoptosis assay*

The apoptotic rate of H9c2 cells were detected by flow cytometry using the annexin V-FITC/propidium iodide (PI) double-labeling method [36]. Cells ($1 \times 10^5$ cells/ml) were seeded in 6-well plates, and were treated with luteolin as described above. Apoptotic cells were then trypsinized and collected by centrifugation at 1000 rpm for 5 min. After washing with PBS, cells were then double-stained using an annexin V-FITC apoptosis detection kit [37]. According to the manufacturer's protocol, cells resuspended in annexin V-FITC binding buffer, were incubated with annexin V-FITC (at a final concentration of 1 μg/ml) for 15 min at room temperature in the dark, and were then incubated with PI (10 μg/ml final concentration). Samples were analyzed with a flow cytometer (Becton Dickinson, Mountain View, CA, USA) by two parameter dot-plots. A total of 10,000 cells were recorded in each case.

H9c2 cells were seeded in the 6-well plates. When they grew to approximately 80% confluence, cells were washed and serum deprived in the presence and absence of H/R injury. At the end of the incubation period, cells were fixed with 4% paraformaldehyde solution for 30 min at room temperature, washed twice with PBS and stained with a Hoechst 33258 staining solution (Beyotime) for 5 min at room temperature and observed by fluorescence microscopy (Olympus IX81) [38,39], with excitation wavelength at 350 nm and emission wavelength at 460 nm.

*P38 and JNK MAPK inhibitor treatment*

To assess the role of MAPK signaling pathway on the H/R induced H9c2 cell apoptosis, H9c2 cells were pretreated for 1 h with 10 μM of

p38 MAPK inhibitor (SB203580) and JNK MAPK inhibitor (SP600125) [40], thereafter, cells were treated in the presence and absence of 30 μM luteolin for additional 24 h, and then, H9c2 cells were suffered with H/R injury for 6 h/5 h, and the ROS generation was measured with DCFH-DA as above; the cell viability was measured using CCK-8 and caspase-3 activation levels were quantified using western blotting.

### *Statistical analysis*

Statistical analysis was performed by using SPSS 10.0. Data are expressed as means ± SD. One-factor analysis of variance was performed when more than two groups were compared, and when significant ($P < 0.05$); Scheffe's test was applied to test for differences between individual groups. $P$ value < 0.05 was considered statistically significant.

## Results

### *Luteolin restores cardiac function and decreases infarct size after I/R injury in rats*

The electrocardiogram data in Table 1 shows that I/R injury significantly decreased the heart rate and peak worth compared with the sham group, while pretreatment with luteolin can increase the heart rate and peak worth dose-dependently. The resulting hemodynamic parameters also showed significant differences in LVSP, LVEDP and ± $dp/dt_{max}$ in the I/R group compared with the sham group; the LVSP, LVEDP and ± $dp/dt_{max}$ in the I/R group were clearly lower while pro-treated with luteolin, which can ameliorate the cardiac function dose-dependently.

Representative images of infarct size as stained by TTC are shown in Fig. 1. Myocardial tissue slices from the sham group exhibited no evidence of infarction (Fig. 1A). In contrast, noticeable infarct areas were observed in myocardial tissue slices of the I/R group (Fig. 1B). This effect was abolished by luteolin treatment, particularly at 70 mg/kg (Fig. 1E). Quantitative analysis of the infarct area further confirms the result.

### *Luteolin protect the I/R injury in myocardial Ultra structure*

The ultra structure of cardiac muscle cells in each condition was examined, the representative electron micrograms are presented in Fig. 2. In the sham group (A and F), cardiac myofibrils stood regularly arranged with well-preserved myofilaments, and mitochondria occupied the cytoplasm between myofibrils with densely packed cristae. The I/R challenge provoked dramatic injury in cardiac muscle cells (B and G), as indicated by disrupted myofibrils and ruptured mitochondria. Pretreatment with luteolin at each of the three doses attenuated the ultra structural alterations induced by I/R (C, D, E and H, I, J).

### *Luteolin reduces LDH, CK, T-SOD, MDA release after I/R injury in rats*

Leakage of CK and LDH from myocardial tissues to blood is indicator of acute myocardial infarction. Treatment with luteolin at dosages of 10–70 mg/kg resulted in a dose-dependent decreased the release of LDH, CK as compared with the I/R group (Table 2).

In MDA and T-SOD activity assay, to exclude the possibility that pro-treated with luteolin may affect the lipid peroxidation and oxidative stress in I/R injury, the absorbance was measured and result showed that MDA level was decreased and T-SOD activity was increased in a dose-dependent manner by luteolin treatment in I/R. At 70 mg/kg of luteolin, T-SOD activity increased and LDH, CK, MDA level decreased markedly.

### *Luteolin affected the MAPK pathway after I/R injury*

Since luteolin treatment improved the oxidative system, we further explored whether luteolin affected the MAPK intracellular signal transduction cascade which has a meaningful role as a regulator of cell function or as signaling molecules activated by ROS. Our western blot data showed that the expression of ERK1/2 was increased in the luteolin group as compared with the I/R group. Ischemia reperfusion injury increased phospho-p38 MAPK/p38 MAPK ratio and phospho-JNK/JNK ratio, but luteolin treatment was able to ameliorate the pathological states (Fig. 3).

### *Luteolin protect hypoxia/reoxygenation injury by affecting oxidation system in H9c2 cell*

Compared with the control group, DCF fluorescence of cardiomyocytes was markedly enhanced in H/R group, indicating an enhancement of ROS level induced by H/R. Pretreatment with luteolin at 30 μM significantly inhibited the DCF fluorescence of myocytes during the reperfusion.

To further determine whether NADPH oxidase activation was accompanied by an increase in NADPH oxidase subunit p47-phox expression, we measured p47-phox protein expression by western blot in H9c2 cells exposed to H/R (6 h/5 h) with or without the treatment of luteolin (30 μM) for 24 h. Quantitative analysis showed that H/R produced an increase in p47-phox protein compared with control and luteolin treatment group (Fig. 4B).

Manganese superoxide dismutase (Mn-SOD), heme oxygenase-1 (HO-1) and heat shock proteins 27 (HSP27) gene transcription regulation signaling pathways involved in the antioxidant defense system. By the Fig. 4C shows, H/R treated H9c2 cells, Mn-SOD mRNA decreased significantly, while the luteolin 30 μM group Mn-SOD mRNA levels, compared with model group, increased significantly. Whereas no effect was observed in the mRNA expression of HO-1 and HSP27 after H/R injury, but treated with luteolin 30 μM can increase these gene expression markedly.

**Table 1.**
Effects of luteolin on cardiac functions after myocardial ischemia-reperfusion injury($n = 6$, $x \pm s$).

| Group | Dose (mg/kg) | Heart rate ($min^{-1}$) | | | Peak worth (mV) | | | LVSP (mm Hg) | LVEDP (mm Hg) | $+dp/dt_{max}$ (mm Hg/s) | $-dp/dt_{max}$ (mm Hg/s) |
|---|---|---|---|---|---|---|---|---|---|---|---|
| | | Normal | After ischemia | After reperfusion | Normal | After ischemia | After reperfusion | | | | |
| Sham | | 487 ± 18 | 469 ± 41 | 470 ± 15 | 0.98 ± 0.07 | 0.86 ± 0.07 | 0.84 ± 0.12 | 96 ± 9 | 3.6 ± 1.5 | 6827 ± 547 | 5624 ± 705 |
| Model | | 499 ± 50 | 425 ± 64$^{\#\#\#}$ | 346 ± 34$^{\#\#}$ | 0.96 ± 0.12 | 0.62 ± 0.08$^{\#}$ | 0.65 ± 0.14$^{\#}$ | 52 ± 11$^{\#\#\#}$ | 8.3 ± 1.8$^{\#\#\#}$ | 5596 ± 746$^{\#\#\#}$ | 4697 ± 658$^{\#\#\#}$ |
| Luteolin | 10 | 489 ± 95 | 413 ± 24 | 376 ± 64 | 1.03 ± 0.29 | 0.69 ± 0.18 | 0.83 ± 0.27$^{*}$ | 56 ± 8 | 7.9 ± 2.2 | 5624 ± 479 | 4812 ± 879 |
| | 40 | 513 ± 79 | 432 ± 19 | 368 ± 57$^{**}$ | 1.07 ± 0.11 | 0.76 ± 0.29$^{\#\#\#}$ | 0.84 ± 0.07$^{**}$ | 62 ± 9$^{**}$ | 6.4 ± 0.9$^{**}$ | 6014 ± 745$^{*}$ | 5126 ± 348$^{**}$ |
| | 70 | 488 ± 30 | 421 ± 12 | 398 ± 37$^{***}$ | 0.96 ± 0.19 | 0.78 ± 0.19$^{\#\#\#}$ | 0.90 ± 0.21$^{**}$ | 82 ± 13$^{***}$ | 4.8 ± 1.2$^{***}$ | 6345 ± 358$^{**}$ | 5469 ± 624$^{***}$ |

Rats in luteolin-treated groups were pretreated with intragastric administration of luteolin for 5 days prior to the myocardial ischemia/reperfusion. Rats in the sham-operated and model groups received vehicle in an identical fashion to the drug-treated groups instead. Myocardial ischemia/reperfusion was induced by LAD ligation. Effects of luteolin on myocardial ischemia–reperfusion injury affect heart rate and peak worth by ECG and the difference in hemodynamic parameters. Left ventricular systolic pressure (LVSP), left ventricular end-diastolic pressure (LVEDP), maximum rate of left ventricular pressure rise ($+dp/dt_{max}$) and maximum rate of left ventricular pressure decline ($-dp/dt_{min}$). Data were expressed as the mean ± SD. $^{\#}P < 0.05$, $^{\#\#\#}P < 0.001$ vs. sham; $^{*}P < 0.05$, $^{**}P < 0.01$, $^{***}P < 0.001$ vs. model group.

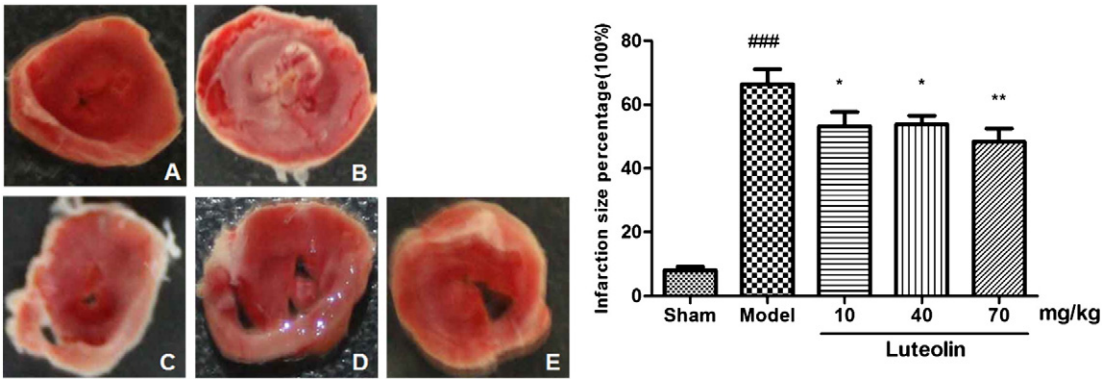


**Fig. 1.** Infarction size of hearts during ischemia/reperfusion. A) Sham group, B) model group, C) luteolin 10 mg/kg, D) luteolin 40 mg/kg, E) luteolin 70 mg/kg. B–E, hearts were subjected to in vivo regional ischemia (30 min)/reperfusion (1 h), and TTC staining to assess the extent of myocardial necrosis. Bars represent the percent of ischemic area at risk in hearts. Values are means ± SD, $n = 6$ per group. $^{###}P < 0.001$ vs. sham; $^{*}P < 0.05$, $^{**}P < 0.001$ vs. model.

*Luteolin attenuated H/R induced H9c2 cell apoptosis*

H/R injury finally induced apoptosis, since the MAPK signaling pathway was activated by H/R. The nuclear morphology was observed under a fluorescence microscope via Hoechst 33,258 staining, the normal group nucleus was stained in the typical shape, round or oval nucleus; H/R injury showed apoptotic nuclei typical of karyopycnosis stain, with chromatin concentrated fragmentation; in the luteolin treated group, the number of cells with apoptotic morphology was significantly less than in the model group (Fig. 5A). Quantitative analysis using flow cytometry confirmed that luteolin significantly inhibited H/R-induced apoptosis (Fig. 5B).

To determine whether luteolin affects H/R-induced caspase 3, 8, and 9 cleavages, we treated cells with H/R in the presence and absence of luteolin and analyzed their cleavages using anti-caspase 3, 8, and 9 antibodies. As shown in Fig. 5C, H/R induced caspase-3, -8, and -9 cleavages in H9c2 cells but the effects were inhibited by luteolin, further demonstrating that luteolin suppressed H/R-induced apoptosis.

To further clarity the mechanism underlying the effect of ROS on MAPK intracellular signal transduction cascade was examined. The activation of p38 MAPK, ERK1/2, and JNK was detected by western blot. The phosphorylation of p38 MAPK and JNK were significantly enhanced and phosphorylation of ERK1/2 was decreased in the H/R group, demonstrating that pretreatment with luteolin 30 μM can ameliorate the phosphorylation levels (Fig. 5D).

*Luteolin restored H/R blocked mitochondrial membrane potential*

From the ultra structure of cardiac muscle cells of rat hearts, we know the mitochondrial damage was recovered by luteolin pretreatment. To determine whether it plays an equal role in H9c2 cells, the mitochondrial membrane potential was studied. Untreated cells exhibited bright-staining mitochondria that emitted red fluorescence. H/R treatment caused the formation of monomeric JC-1, indicative of loss of membrane potential. Luteolin pretreatment, however, blocked the H/R-induced formation of JC-1 monomers (Fig. 6), suggesting luteolin can restore H/R-induced loss of mitochondrial membrane potential.

*Inhibition of p38 MAPK and JNK activation implicated in the protection of luteolin against H/R induced reactive oxygen species and apoptosis in H9c2 cells*

As shown in Fig. 7A and B, pretreatment with 30 μM luteolin for 24 h before H9c2 cells suffered with 6 h/5 h H/R injury clearly ameliorated ROS accumulation and the cell viability. Similarly, pretreatment of cells with 10 μM SB203580 (a selective inhibitor of p38) and

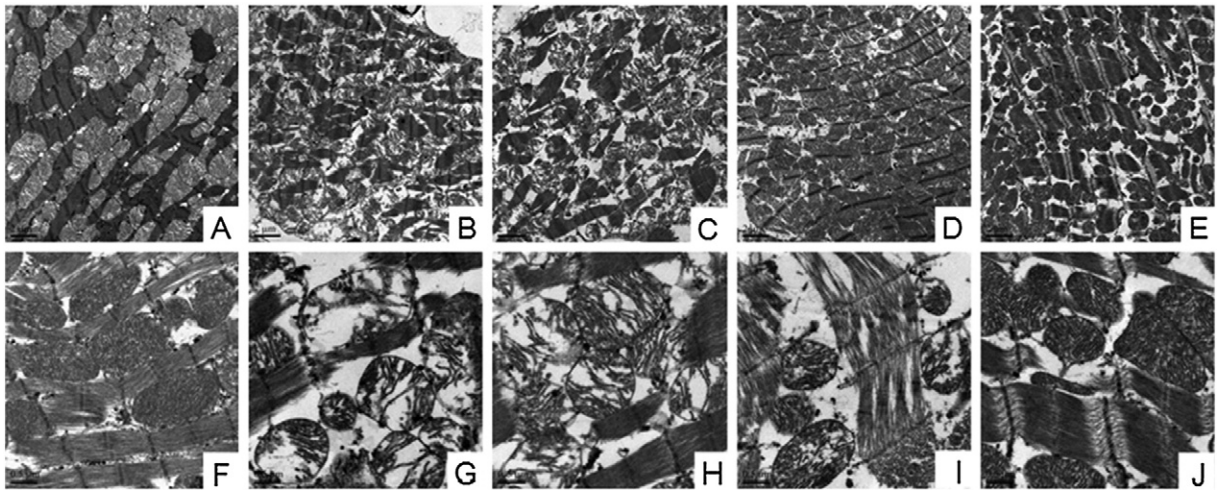


**Fig. 2.** Ultrastructural observation of LAD ligation-induced ischemic myocardium in rats. Myocardial ischemia was induced by LAD ligation. Tissues of the surrounding infarction areas of the left ventricle were stained and observed under a transmission electronic microscope. (A, F) Sham-operated group: cardiac myofibrils stood regularly arranged with well-preserved myofilaments, and mitochondria occupied the cytoplasm between myofibrils with densely packed cristae. (B, G) Model group: the myocardial fiber was disordered, even dissolved. The mitochondria were enlarged, even exhibiting vacuolar degeneration. (C, H 10 mg/kg, D, I 40 mg/kg, E, J 70 mg/kg) luteolin-treated group: the ultrastructural changes of myocytes were extensively attenuated. Mitochondria and myocardial fiber showed slight edema. A–E was 5000×, bar = 2 μm, F–J was 15,000×, bar = 0.5 μm.

**Table 2.**
Effects of luteolin on the biochemical parameters in serum of rats with ischemia/reperfusion injury myocardial ($n = 6, x \pm s$).

| Group | Dose (mg/kg) | n | LDH (U/ml) | CK (U/ml) | MDA (μM/ml) | T-SOD (U/ml) |
|---|---|---|---|---|---|---|
| Sham | | 6 | 0.11 ± 0.01 | 0.99 ± 0.15 | 5.33 ± 1.84 | 52.34 ± 2.24 |
| Model | | 6 | 0.14 ± 0.02$^{\#\#}$ | 1.72 ± 0.35$^{\#\#\#}$ | 10.00 ± 4.21$^{\#\#}$ | 48.06 ± 2.48$^{\#\#\#}$ |
| | 10 | 6 | 0.13 ± 0.02 | 1.47 ± 0.12 | 6.27 ± 4.07$^{*}$ | 50.87 ± 3.10$^{**}$ |
| Luteolin | 40 | 6 | 0.12 ± 0.01$^{*}$ | 1.23 ± 0.27$^{**}$ | 5.46 ± 1.46$^{**}$ | 52.12 ± 2.91$^{**}$ |
| | 70 | 6 | 0.12 ± 0.02$^{*}$ | 1.22 ± 0.19$^{**}$ | 5.33 ± 9.71$^{**}$ | 52.55 ± 1.40$^{***}$ |

Rats in luteolin treated groups were pretreated with intragastric administration of luteolin for 5 days prior to the myocardial ischemia/reperfusion. Rats in the sham-operated and model groups received vehicle in an identical fashion to the drug-treated groups instead. Myocardial ischemia/reperfusion was induced by LAD ligation. LDH, CK, and T-SOD activities and MDA levels in serum were spectrophotometrically determined. Data were expressed as the mean ± SD ($n = 6$). $^{\#\#}P < 0.01$, $^{\#\#\#}P < 0.001$ vs. sham; $^{*}P < 0.05$, $^{**}P < 0.01$, $^{***}P < 0.001$ vs. model group.

SP600125 (a selective inhibitor of JNK) for 60 min also markedly decreased the H/R-induced ROS generation and cytotoxicity. As shown in Fig. 7C, H9c2 cells suffering 6 h/5 h H/R injury caused an obvious activation of caspase-3. In contrast, pretreatment of cells with 30 μM luteolin for 24 h and 10 μM SB203580, SP600125 for 60 min markedly decreased the H/R-induced caspase-3 activation. 10 μM SB203580, SP600125 alone had no effect on the oxidative system and apoptosis of H9c2 cells. These findings showed that the activation of p38 MAPK and JNK were implicated in H/R-triggered cytotoxicity and that luteolin may protect against H/R-induced cytotoxicity may by inhibiting the activation of p38 MAPK and JNK in H9c2 cells.

## Discussion

This study demonstrated that MIRI activated myocardial ROS–MAPK pathway and induced apoptosis, whereas luteolin pretreatment resulted in attenuation of the oxidant system and the apoptosis factor, and affected the MAPK pathway. The cardio protection of luteolin against MIRI may be due to the suppression of the ROS–MAPK via mitochondrial protection.

Ischemia disturbs the balance between the formation and elimination of reactive oxygen species (ROS), resulting in the accumulation of ROS. Excessive ROS reacts with excessive endogenous NO to form the neurotoxin peroxynitrite. The endogenous defense system, primarily the antioxidant enzyme system (eg, SOD and GSH-PX), is critical to attenuating the injury induced by ischemia/reperfusion [41]. Significantly increased levels of MDA (the product of lipid peroxidation) in the I/R group indicated severe oxidative damage caused by ischemia/reperfusion injury [42]. Following reperfusion, CK shows an early and rapid rise to a high maximum value with rapid normalization. LDH is a late release following myocardial infarction. LDH and CK are serum biomarkers that reflects myocardial damage, SOD and MDA are important indexes of myocardial oxidative damage. Luteolin dose-dependently lowered the increased levels of MDA, LDH and CK. Moreover, luteolin enhanced the activity of the antioxidase level of T-SOD, compared with the I/R group, but 10 mg/kg of luteolin had no visible effect on CK and LDH release, we suppose that 10 mg/kg can affect the oxidative system. These biological parameters demonstrated the protective ability of luteolin against ischemia/reperfusion injury in vivo by mediating reactive oxygen species.

MIRI induces mitochondrial injury by generating oxygen free radicals [43]. Our results provided quantitative data that support the assumption that pretreatment with luteolin can protect mitochondrial function and decrease SOD activities and oxidative stress to reduce myocardial I/R injury. Mitochondria are organelles for the production of metabolic energy in the form of ATP, and also represent one of the most significant sources of cellular ROS generation, playing a key role in controlling the pathways that lead to cell death [44,45]. Notably, pretreatment with 10, 40, or 70 mg/kg luteolin can significantly protect the mitochondrial ultrastructure of MIRI rats in vivo, and 30 μM luteolin can counteract the H/R induced loss of mitochondrial membrane potential in vitro. Therefore, the role of luteolin in MIRI or H/R injury may be mitochondrial protection to mediate the oxidative system and apoptosis.

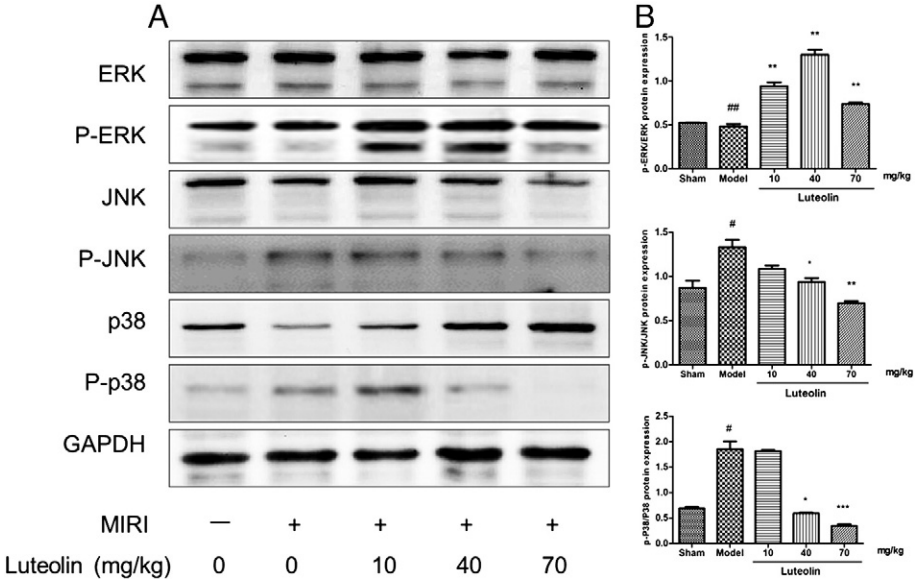


**Fig. 3.** The effects of luteolin on MAPK pathway of LAD ligation-induced myocardial ischemia/reperfusion injury of rat. A: the representative western blotting picture of the MAPK protein in the sham group, I/R group, luteolin 10 mg/kg + I/R group, luteolin 40 mg/kg + I/R group, luteolin 70 mg/kg + I/R group. B: semiquantitative analysis of MAPK protein content. Values are means ± SD from 6 animals. $^{\#}P < 0.05$, $^{\#\#}P < 0.01$ vs. sham group, $^{*}P < 0.05$, $^{**}P < 0.01$, $^{***}P < 0.001$ vs. model group.

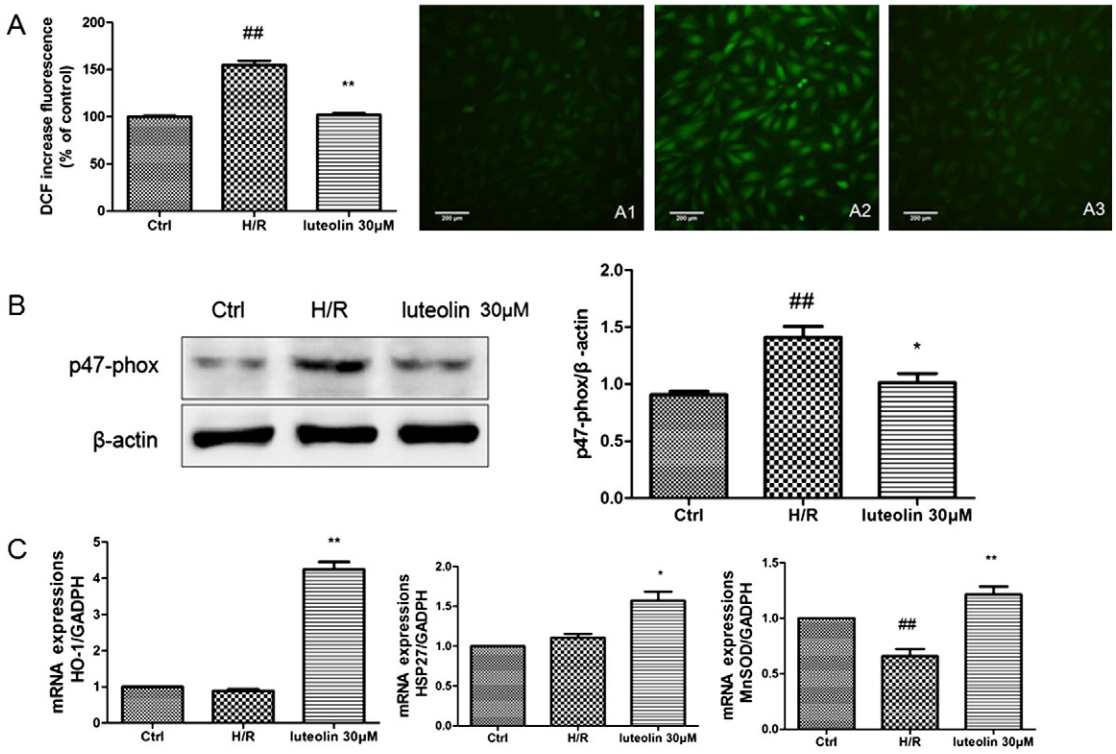


**Fig. 4.** Effects of luteolin pretreatment on hypoxia/reoxygenation-induced oxidation system disorder in H9c2 cardiomyocytes. A: intracellular ROS levels were examined of percentage increase of DCF fluorescence by fluorescence microplate reader. Cells were pretreated with different concentrations of luteolin for 24 h, suffered with hypoxia/reoxygenation injury for 6 h/5 h, and incubated with DCFH-DA as the probe oxidized to DCF intracellularly and emitting fluorescence, A1 for control group, A2 for H/R group, A3 for luteolin 30 μM + H/R group. B: Effect of luteolin on the p47-phox expression of NADPH oxidase active subunit in H9c2 cells exposed to H/R. C: Effect of luteolin on the expression of Mn-SOD, HO-1 and HSP27 mRNA levels in H/R suffered H9c2 cells. Each column represents mean ± SD ($n = 3$). $^{\#\#}P < 0.01$ vs. control group, $^{*}P < 0.05$,$^{**}P < 0.01$ vs. model group.

Under ischemia–reperfusion stress response, NOX is stimulated and activated to generate excessive ROS; peroxidation participates in the pathogenesis of injury. Research on protein p47-phox, an important active subunit of NOX, showed that active NOX can increase production of ROS. Our results with the H9c2 H/R model show significant evidence that luteolin can inhibit the protein expression of p47-phox. Reperfusion induced cell death was attenuated by over-expression of Mn-superoxide dismutase (Mn-SOD) or mitochondrial phospholipid hydroperoxide glutathione peroxidase (mito-PHGPx) [46]. Heme-oxygenase-1 (HO-1), a stress-inducible protein, is an important cytoprotective agent against ischemia/reperfusion (I/R) injury, which can generate the majority if not all of the endogenously produced carbon monoxide [47,48]. Heat shock protein 27 (HSP27) is an intracellular stress protein with cytoprotective effects for a variety of noxious stresses [49]. A great deal of research has showed that ROS generation may result in apoptosis during H/R injury, and reduced ROS generation can suppress MIRI via anti-oxidants and anti-oxidative enzymes including Mn-SOD, HO-1 and HSP27 [50]. Our real-time PCR data shows that, luteolin treatment can up-regulate the mRNA expression of Mn-SOD to protect the H/R H9c2 cell, but H/R injury for 6 h h has no effect on the HO-1 and HSP27 mRNA expression, luteolin alone can up-regulate the HO-1 and HSP27 mRNA expression. These data shows that ischemia/reperfusion injury could cause the mitochondrial damage and resulted in the accumulation of reactive oxygen species in vivo. Luteolin 30 μM can significantly decrease the ROS generation and this function may be regulating the Mn-SOD mRNA expression.

Mitogen-activated protein kinase, a family of serine/threonine kinases, can mediate intracellular signals in response to various stimuli. The activation of MAPK pathway, which is linked to oxidative stress, has been demonstrated to be involved in the progression of cell apoptosis [51]. Mammals express at least three distinct groups of MAPKs, including p38 MAPK, ERK1/2 and JNK. ERK1/2 activation involved in cell-survival pathway and plays an important role in the recovery from the damage caused by myocardium ischemia [52]. JNK and p38 participate in MIRI and myocardial apoptosis while antagonizing the expression and phosphorylation of JNK and p38; this can reduce myocardial infarction and apoptosis, restoring cardiac function after myocardial ischemia [53,54]. Similar to these previous studies, our study showed that MIRI and H/R significantly enhanced the expression levels of P-p38 MAPK, P-ERK1/2 and P-JNK, indicating activation of MAPK by MIRI and H/R. Luteolin 10, 40, and 70 mg/kg pretreated rats and 30 μM pretreated H9c2 cells showed significant activation of ERK1/2 phosphorylation and inhibition of P-p38 MAPK and P-JNK. We also examined the role of p38 MAPK activation in H/R-induced injuries. H9c2 cells were pretreated with 10 μM SB203580 (a selective inhibitor p38 MAPK) and SP600125 (a selective inhibitor of JNK) before exposure to H/R for 6 h/5 h. It was shown that SB203580 and SP600125 considerably depressed H/R-induced injuries, mitigating the impact on cell viability and caspase-3 activation. Notably, inhibitory effects of SB203580 and SP600125 on H/R induction of ROS generation were also observed. We have provided clear evidence that luteolin treatment can affect MAPK pathways to protect apoptosis; furthermore, we found a positive interaction between the ROS, MAPK activation and apoptosis: luteolin treatment decreased the ROS generation and stimulation to affect the MAPK pathway, while MAPK activation is an earlier event to caspase activation and apoptosis; MAPK can directly improve apoptotic caspase-3 expression, on the other hand, by affecting the mitochondrial oxidative metabolism and the downstream caspase-9 activation indirectly affects the caspase-3, the final step of the proapoptotic signaling pathway.

In this study, we investigated the protective effects of luteolin in I/R injury animal model and hypoxia/reoxygenation injury model. The results confirmed that luteolin can prevent myocardial damage on I/R challenge via mitochondria protection and the ROS–MAPK pathway.

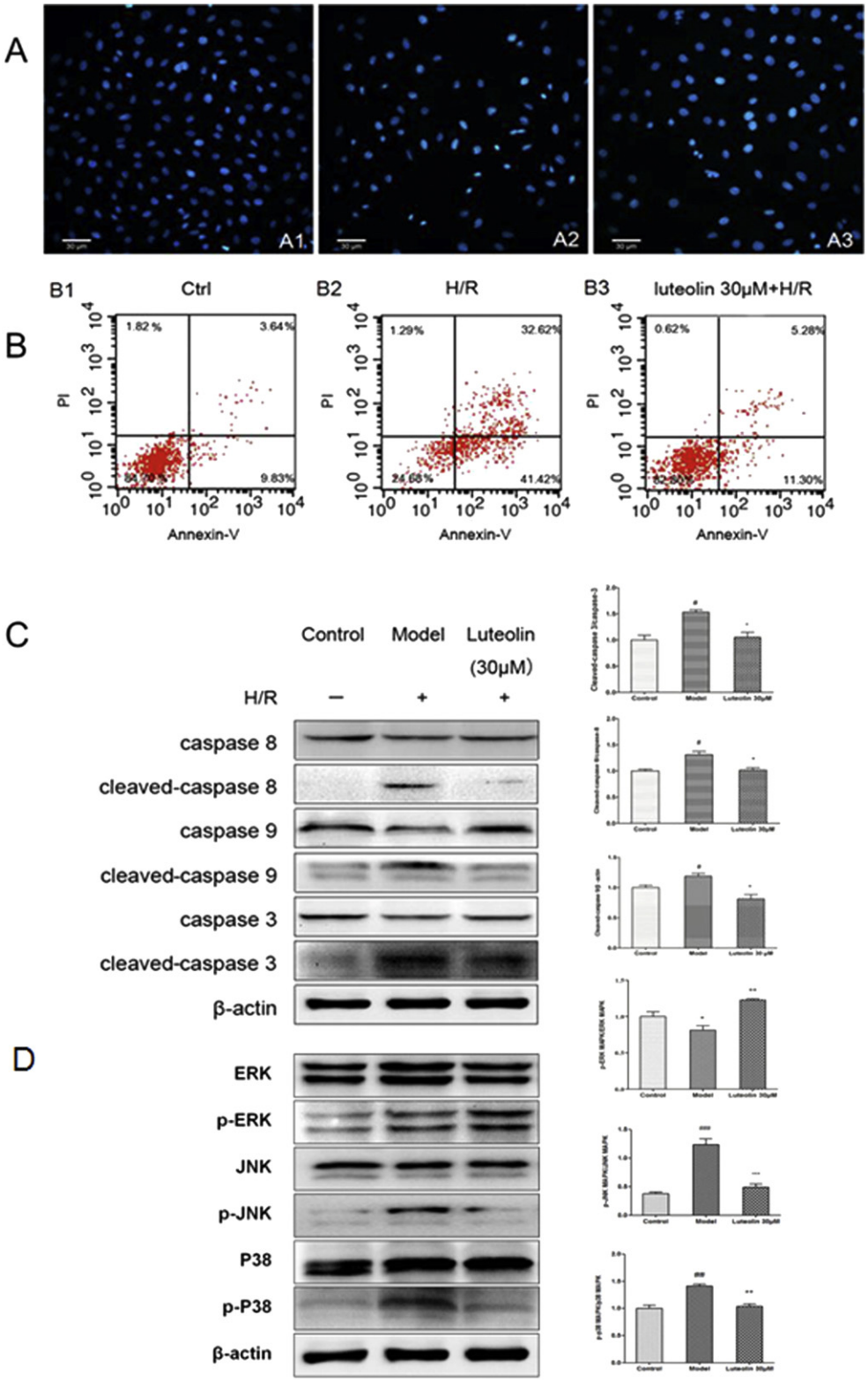


**Fig. 5..** Effects of luteolin pretreatment on hypoxia/reoxygenation induced apoptosis in H9c2 cardiomyocytes. A: The morphological alteration of nuclear of H9c2 after H/R for 6 h/5 h, cells were fixed and stained by Hoechst 33,258 for the determination of apoptosis (original magnification, 200×). B: Flow cytometric detection was performed to detect apoptotic ratio of H9c2 cardiomyocytes in the control, H/R, H/R + luteolin (30 μM) groups. The representative results of flow cytometric detection were shown. C: Western blots showing increased activation of caspase-3, -8, and -9 in H/R suffered H9c2 cells indicating that the apoptosis, treated with luteolin 30 μM for 24 h before H/R, caspase-3, -8, and -9 expression was decreased significantly compared with model group. D: β-actin was used to ensure equal loading of total lysate, images show that cells treated/untreated with luteolin 30 μM affect the MAPK pathway protein expression after H/R injury. The value beneath each protein band in the figure is the relative expression of the specific protein, means ± SD deviation from at least three replicated experiments. $^{\#\#}P < 0.01$ vs. control group, $^{*}P < 0.05$, $^{**}P < 0.01$ vs. model group.

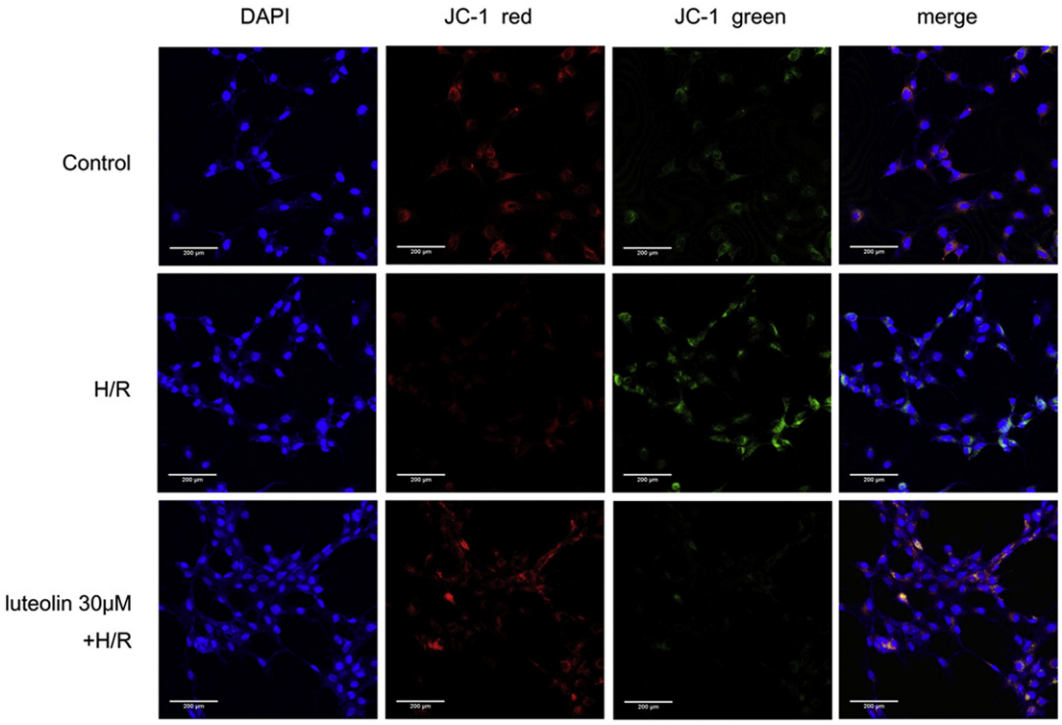


**Fig. 6.** Effects of luteolin pretreatment on hypoxia/reoxygenation-induced changes of mitochondrial membrane potential in H9c2 cardiomyocytes. Cells were treated with luteolin 30 μM for 24 h and subjected to hypoxia/reoxygenation challenge. Mitochondrial membrane potential (ΔΨm) was measured by staining cells with a fluorescent cationic dye JC-1, followed by observation under a confocal laser scanning microscope. JC-1 is a cationic dye that exhibit potential-dependent accumulation in mitochondria, indicated by a fluorescence emission shift from green (~525 nm) to red (~590 nm). In H/R group, mitochondrial depolarization is indicated by a decrease in the red/green fluorescence intensity ratio, and in luteolin group, red/green fluorescence intensity ratio was increased.

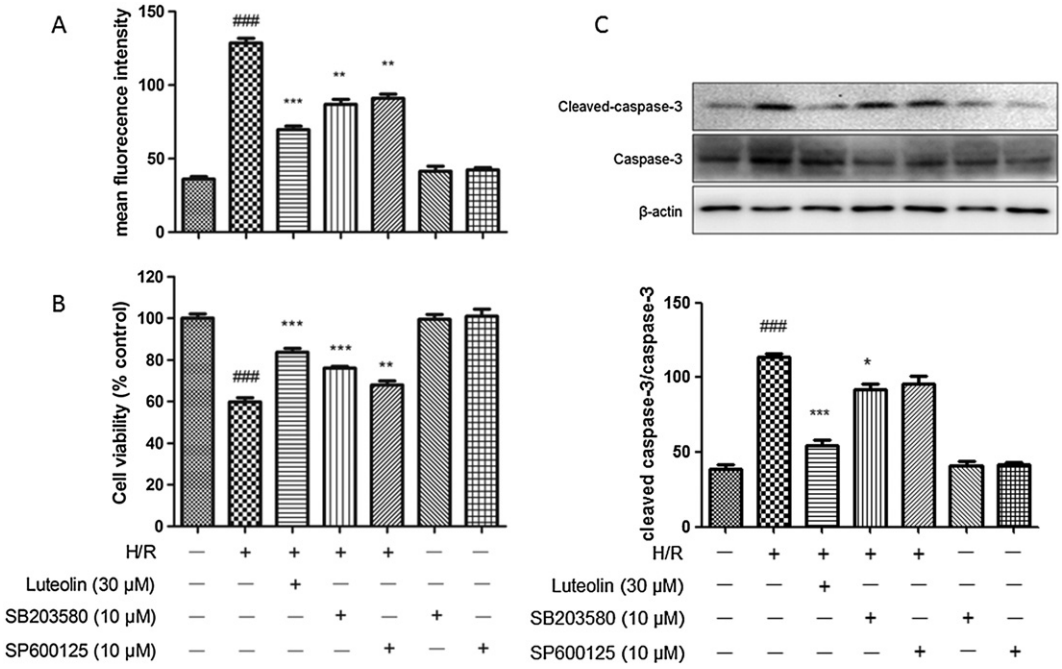


**Fig. 7.** Effects of p38 MAPK and JNK inhibitor pretreatment on hypoxia/reoxygenation induced reactive oxygen species (ROS), cell viability and apoptosis in H9c2 cardiomyocytes. A: Cells were treated with H/R injury for 6 h/5 h in the absence or presence of pre-treatment with either 30 μM luteolin for 24 h or 10 μM SB203580 and SP600125 for 60 min. Quantitative analysis for the mean fluorescence (MFI) of DCFH-DA staining of H9c2 cells by fluorescence microplate reader. B: Cell viability was detected using the cell counter kit (CCK-8). C: Western blots showing increased activation of caspase-3 in H/R suffered H9c2 cells indicating the apoptosis, treated with luteolin 30 μM for 24 h or 10 μM SB203580 and SP600125 for 60 min before H/R, caspase-3 activation was detected. β-Actin was used to ensure equal loading of total lysate. The value beneath each protein band in the figure is the relative expression of the specific protein, means ± SD deviation from at least three replicated experiments. $^{###}P < 0.001$ compared with the control group; $^{*}P < 0.05$, $^{**}P < 0.01$, $^{***}P < 0.001$ compared with H/R-treated group.

This study provides basis for further research of effective substance and mechanism.

## Conclusion

This study demonstrated the efficacy of luteolin in the treatment of myocardial ischemia/reperfusion in vivo and in vitro. The effect may result from mediation of the ROS system and MAPK pathways, which interacts with mitochondrial function, via restraining the phosphorylation of JNK and p38 MAPK, and promoting the activation of ERK1/2, up-regulating the mRNA transcription of Mn-SOD, and ameliorating mitochondrial function. This fact and the safety of luteolin warranted it as an effective therapeutic agent against myocardial ischemia/reperfusion injury.

### Conflict of interest statement

The authors state that there are no conflicts of interest.

## Acknowledgments

This work was supported by the National Natural Science Foundation of China (30873156; 30672524), the New Century Excellent Talents in University (NCET-07–0851), the Mega-projects of Science Research for the 12th Five-Year Plan of China (2011ZX09401-007), the National Science and Technology Infrastructure Program (2012BAI30B001) and the Technological Innovation Team of Jiangsu Higher Education.

## References

[1] S. Mendis, P. Puska, B. Norrving, Global Atlas on Cardiovascular Disease Prevention and Control, World Health Organization, 2011.
[2] J.P. Monassier, Reperfusion injury in acute myocardial infarction. From bench to cath lab. Part I: basic considerations, Arch. Cardiovasc. Dis. 101 (7–8) (2008) 491–500.
[3] M. Rodriguez-Porcel, et al., Functional and structural remodeling of the myocardial microvasculature in early experimental hypertension, Am. J. Physiol. Heart Circ. Physiol. 290 (3) (2006) H978.
[4] A.T. Turer, J.A. Hill, Pathogenesis of myocardial ischemia–reperfusion injury and rationale for therapy, Am. J. Cardiol. 106 (3) (2010) 360–368.
[5] C. Tanaka-Esposito, Q. Chen, E.J. Lesnefsky, Blockade of electron transport before ischemia protects mitochondria and decreases myocardial injury during reperfusion in aged rat hearts, Transl. Res. 160 (3) (2012) 207–216.
[6] M. Murugesan, V. Manju, Luteolin promotes mitochondrial protection during acute and chronic periods of isoproterenol induced myocardial infarction in rats, Egypt. Heart J. 65 (4) (2013) 319–327.
[7] Å.B. Gustafsson, R.A. Gottlieb, Bcl-2 family members and apoptosis, taken to heart, Am. J. Physiol. Cell Physiol. 292 (1) (2007) C45–C51.
[8] L.B. Becker, New concepts in reactive oxygen species and cardiovascular reperfusion physiology, Cardiovasc. Res. 61 (3) (2004) 461–470.
[9] E. Borchi, et al., Enhanced ROS production by NADPH oxidase is correlated to changes in antioxidant enzyme activity in human heart failure, Biochim. Biophys. Acta 1802 (3) (2010) 331–338.
[10] T.M. Scarabelli, et al., Different signaling pathways induce apoptosis in endothelial cells and cardiac myocytes during ischemia/reperfusion injury, Circ. Res. 90 (6) (2002) 745–748.
[11] Y. Son, et al., Mitogen-activated protein kinases and reactive oxygen species: how can ROS activate MAPK pathways? J. Signal Transduct. 2011 (2011).
[12] C. Ferrandi, et al., Inhibition of c-Jun N-terminal kinase decreases cardiomyocyte apoptosis and infarct size after myocardial ischemia and reperfusion in anaesthetized rats, Br. J. Pharmacol. 142 (6) (2004) 953–960.
[13] J. Li, et al., AMP-activated protein kinase activates p38 mitogen-activated protein kinase by increasing recruitment of p38 MAPK to TAB1 in the ischemic heart, Circ. Res. 97 (9) (2005) 872–879.
[14] L. Yuan, et al., MAPK signaling pathways regulate mitochondrial-mediated apoptosis induced by isoorientin in human hepatoblastoma cancer cells, Food Chem. Toxicol. 53 (2013) 62–68.
[15] A. Taliou, et al., An open-label pilot study of a formulation containing the anti-inflammatory flavonoid luteolin and its effects on behavior in children with autism spectrum disorders, Clin. Ther. 35 (5) (2013) 592–602.
[16] V. Manju, V. Balasubramaniyan, N. Nalini, Rat colonic lipid peroxidation and antioxidant status: The effects of dietary luteolin on 1, 2-dimethylhydrazine challenge, Cell. Mol. Biol. Lett. 10 (3) (2005) 535.
[17] Y. Lin, et al., Luteolin, a flavonoid with potentials for cancer prevention and therapy, Curr. Cancer Drug Targets 8 (7) (2008) 634.
[18] L. Qi, et al., Luteolin improves contractile function and attenuates apoptosis following ischemia-reperfusion in adult rat cardiomyocytes, Eur. J. Pharmacol. 668 (1–2) (2011) 201–207.
[19] K.E. Eblin, et al., Reactive oxygen species regulate properties of transformation in UROtsa cells exposed to monomethylarsonous acid by modulating MAPK signaling, Toxicology 255 (1–2) (2009) 107–114.
[20] J. Ravindran, et al., Modulation of ROS/MAPK signaling pathways by okadaic acid leads to cell death via, mitochondrial mediated caspase-dependent mechanism, Apoptosis 16 (2) (2011) 145–161.
[21] A. Kulisz, et al., Mitochondrial ROS initiate phosphorylation of p38 MAP kinase during hypoxia in cardiomyocytes, Am. J. Physiol. Lung Cell. Mol. Physiol. 282 (6) (2002) L1324–L1329.
[22] S.A. Samsamshariat, Z.A. Samsamshariat, M.R. Movahed, A novel method for safe and accurate left anterior descending coronary artery ligation for research in rats, Cardiovasc. Revasc. Med. 6 (3) (2005) 121–123.
[23] J.W. Kim, et al., Daidzein administration in vivo reduces myocardial injury in a rat ischemia/reperfusion model by inhibiting NF-kappaB activation, Life Sci. 84 (7–8) (2009) 227–234.
[24] H.-L. Wu, et al., 5-HT1A/1B receptors as targets for optimizing pigmentary responses in C57BL/6 mouse skin to stress, PLoS One 9 (2) (2014) e89663.
[25] X.K. Qu, et al., Utility of 64-MSCT in assessing acute non-reperfused myocardial infarct size, J. Geriatr. Cardiol. 10 (3) (2013) 247–252.
[26] K.A. Webster, D.J. Discher, N.H. Bishopric, Cardioprotection in an *in vitro* model of hypoxic preconditioning, J. Mol. Cell. Cardiol. 27 (1) (1995) 453–458.
[27] T. Asakawa, S. Matsushita, Thiobarbituric acid test for detecting lipid peroxides, Lipids 14 (4) (1979) 401–406.
[28] W. Flameng, et al., Ultrastructural and cytochemical correlates of myocardial protection by cardiac hypothermia in man, J. Thorac. Cardiovasc. Surg. 79 (3) (1980) 413–424.
[29] X. Xu, R. Bucala, J. Ren, Macrophage migration inhibitory factor deficiency augments doxorubicin-induced cardiomyopathy, J. Am. Heart Assoc. 2 (6) (2013) e000439.
[30] N. Zhao, et al., Cardiotonic pills, a compound Chinese medicine, protects ischemia-reperfusion-induced microcirculatory disturbance and myocardial damage in rats, Am. J. Physiol. Heart Circ. Physiol. 298 (4) (2010) H1166–H1176.
[31] Y. Tian, A. Daoud, J. Shang, Effects of bpV(pic) and bpV(phen) on H9c2 cardiomyoblasts during both hypoxia/reoxygenation and $H_2O_2$-induced injuries, Mol. Med. Rep. 5 (3) (2012) 852–858.
[32] P.Y. Chiu, et al., Schisandrin B stereoisomers protect against hypoxia/reoxygenation-induced apoptosis and inhibit associated changes in $Ca^{2+}$-induced mitochondrial permeability transition and mitochondrial membrane potential in H9c2 cardiomyocytes, Life Sci. 82 (21–22) (2008) 1092–1101.
[33] Y.Y. Tian, et al., Catalpol protects dopaminergic neurons from LPS-induced neurotoxicity in mesencephalic neuron–glia cultures, Life Sci. 80 (3) (2006) 193–199.
[34] C.L. Andersen, J.L. Jensen, T.F. Ørntoft, Normalization of real-time quantitative reverse transcription-PCR data: a model-based variance estimation approach to identify genes suited for normalization, applied to bladder and colon cancer data sets, Cancer Res. 64 (15) (2004) 5245–5250.
[35] M.M. Siddique, et al., Ablation of dihydroceramide desaturase confers resistance to etoposide-induced apoptosis in vitro, PLoS One 7 (9) (2012) e44042.
[36] G. Brumatti, C. Sheridan, S.J. Martin, Expression and purification of recombinant annexin V for the detection of membrane alterations on apoptotic cells, Methods 44 (3) (2008) 235–240.
[37] H.L. Yan, et al., Repression of the miR-17–92 cluster by p53 has an important function in hypoxia-induced apoptosis, EMBO J. 28 (18) (2009) 2719–2732.
[38] M.H. Bao, et al., Rutaecarpine prevents hypoxia-reoxygenation-induced myocardial cell apoptosis via inhibition of NADPH oxidases, Can. J. Physiol. Pharmacol. 89 (3) (2011) 177–186.
[39] Y.F. Lin, et al., Recombinant tissue factor pathway inhibitor induces apoptosis in cultured rat mesangial cells via its Kunitz-3 domain and C-terminal through inhibiting PI3-kinase/Akt pathway, Apoptosis 12 (12) (2007) 2163–2173.
[40] P.Y. Chiu, et al., Schisandrin B elicits a glutathione antioxidant response and protects against apoptosis via the redox-sensitive ERK/Nrf2 pathway in H9c2 cells, Mol. Cell. Biochem. 350 (1–2) (2011) 237–250.
[41] H. Jaeschke, B.L. Woolbright, Current strategies to minimize hepatic ischemia-reperfusion injury by targeting reactive oxygen species, Transplant. Rev. (Orlando) 26 (2) (2012) 103–114.
[42] Z. Cheng, et al., Cordycepin protects against cerebral ischemia/reperfusion injury in vivo and in vitro, Eur. J. Pharmacol. 664 (1–3) (2011) 20–28.
[43] E. Murphy, C. Steenbergen, Mechanisms underlying acute protection from cardiac ischemia–reperfusion injury, Physiol. Rev. 88 (2) (2008) 581–609.
[44] S. Desagher, J.-C. Martinou, Mitochondria as the central control point of apoptosis, Trends Cell Biol. 10 (9) (2000) 369–377.
[45] S.I. Dikalov, Z. Ungvari, Role of mitochondrial oxidative stress in hypertension, Am. J. Physiol. Heart Circ. Physiol. 305 (10) (2013) H1417–H1427.
[46] G. Loor, et al., Mitochondrial oxidant stress triggers cell death in simulated ischemia–reperfusion, Biochim. Biophys. Acta 1813 (7) (2011) 1382–1394.
[47] A.S. Pachori, et al., Heme-oxygenase-1-induced protection against hypoxia/reoxygenation is dependent on biliverdin reductase and its interaction with PI3K/Akt pathway, J. Mol. Cell. Cardiol. 43 (5) (2007) 580–592.
[48] L.E. Otterbein, A.M. Choi, Heme oxygenase: colors of defense against cellular stress, Am. J. Physiol. Lung Cell. Mol. Physiol. 279 (6) (2000) L1029–L1037.
[49] J.H. Kwon, et al., Protective effect of heat shock protein 27 using protein transduction domain-mediated delivery on ischemia/reperfusion heart injury, Biochem. Biophys. Res. Commun. 363 (2) (2007) 399–404.
[50] K. Terui, et al., Stat3 confers resistance against hypoxia/reoxygenation-induced oxidative injury in hepatocytes through upregulation of Mn-SOD, J. Hepatol. 41 (6) (2004) 957–965.

[51] A. Lan, et al., Hydrogen sulfide protects against chemical hypoxia-induced injury by inhibiting ROS-activated ERK1/2 and p38MAPK signaling pathways in PC12 cells, PLoS One 6 (10) (2011) e25921.
[52] H. Wang, et al., Pioglitazone attenuates myocardial ischemia-reperfusion injury via up-regulation of ERK and COX-2, Biosci. Trends 6 (6) (2012) 325–332.
[53] J.W. Chambers, et al., Inhibition of JNK mitochondrial localization and signaling is protective against ischemia/reperfusion injury in rats, J. Biol. Chem. 288 (6) (2013) 4000–4011.
[54] S. Akhtar, et al., Activation of EGFR/ERBB2 via pathways involving ERK1/2, P38 MAPK, AKT and FOXO enhances recovery of diabetic hearts from ischemia–reperfusion injury, PLoS One 7 (6) (2012) e39066.